Applied Chemical Engineering (2024) Volume 7 Issue 4 ISSN: 2578-2010 (O)
doi: 10.59429/ace.v7i4.5579

ORIGINAL RESEARCH ARTICLE

Synthesis of triclosan-derived coumarins as potent, biocompatible, broad-spectrum antimicrobial agents

Marwa Mohammed Alshaher, Yasser Fakri Mustafa*

Department of Pharmaceutical Chemistry, College of Pharmacy, University of Mosul, Mosul, 41001, Iraq

***Corresponding author:** Dr.yassermustafa@uomosul.edu.iq

ABSTRACT

Objective: Various personal care products previously used triclosan, a chlorinated antimicrobial agent. However, safety and environmental concerns have grown, forbidding its application. Given this fact, the present work aims to repurpose this out-of-use chemical by including it as a precursor for synthesizing nineteen triclosan-based coumarins (TBCs). **Methods:** The spectrophotometric methods applied to confirm the chemical structures of TBCs were FTIR, ^{1}H-NMR, ^{13}C-NMR, and HRMS. The antimicrobial investigations were run through using broth microdilution methodology and many pathogenic microbes. These include six aerobic and four anaerobic ATCC-approved bacterial strains, as well as two fungal strains. We validated the results by comparing them with three standards: ciprofloxacin, metronidazole, and nystatin, which were based on the tested microbe. On the other hand, the biocompatibility investigations determined the ability of TBCs to inhibit the normal growth of three microbiome strains. **Results:** The results revealed several conclusive points, including the bactericidal impact of the synthesized TBCs on both pathogenic and microbiome strains tested, with low and high MIC values, respectively. The impact of the synthesized TBCs on pathogenic bacteria was dependent on the number and type of substitutes on the D ring, but this was not the case for microbiome bacteria, where these two factors were of low importance. These factors also influence the activity of the synthesized TBCs against pathogenic fungi. The latter microbes exhibit a high level of sensitivity to the synthetic intermediate, which contains a carboxylic acid moiety within its structure. We concluded from these findings that the number of chlorides that deactivated the D ring directly promoted the anti-aerobic bacterial activity. The same holds true for the anti-anaerobic bacteria, albeit with the addition of nitro groups. **Conclusion:** the results could provide insights into how the structure of the synthesized TBCs influences their antimicrobial activity. This renders them highly promising as potential future medicines that are robust, safe, and effective against a broad spectrum of microbes.

Keywords: coumarin; triclosan; antibacterial; antifungal; biocompatibility

ARTICLE INFO

Received: 10 December 2024
Accepted: 19 December 2024
Available online: 25 December 2024

1. Introduction

Triclosan, a synthetic chlorophenolic compound with broad-spectrum antimicrobial qualities, can be found in many different kinds of personal care and beauty products[1]. From its first development in 1972 to its widespread use in personal hygiene and healthcare goods since then, triclosan has been marketed for these qualities and has been utilized widely to mitigate or avoid bacterial growth[2]. Triclosan has become a widely debated and scrutinized topic, despite its effective bacterial killing and growth limitation capabilities. Scientists are concerned about its impact on human health, particularly its potential to disrupt thyroid hormone regulation and exacerbate the issue of antibiotic resistance[3]. Furthermore, research has demonstrated that triclosan can accumulate in water systems and other environmental areas, posing a threat to aquatic life and ecosystems[4]. The lack of

adequate proof of triclosan's effectiveness compared to conventional soap and water has led government agencies like the American Food and Drug Administration to prohibit its inclusion in generic hand soaps and body washes. This move is in reaction to these concerns[5]. Numerous companies are choosing to eliminate triclosan from their formulations due to public and humanitarian demands for safer alternatives. Although certain products, like toothpaste, still include the chemical under study, this trend is swiftly shifting[6].

Tonka beans, cinnamon, and sweet clover are just a few of the many plant sources of coumarins, a class of nature-derived products with a distinctively sweet fragrance[7]. Structurally related to benzopyrone chemicals, coumarins naturally shield plants from harmful chemicals and insects, playing a crucial role in their defense systems[8]. Numerous well-developed synthetic methods, including a variety of organic and inorganic agents, catalyze the synthesis of coumarins in the chemical sciences[9–11]. The wide variety of biological and pharmacological effects of coumarins has also piqued their interest[12]. Their ability to prevent blood clots is what inspired the creation of medications like warfarin[13]. In addition to this ability, medicinal chemists are also studying coumarins for their antioxidant[14,15], anti-inflammatory[16,17], hypoglycemic[18,19], hypolipidemic[20,21], antibacterial[22,23], anticancer[24,25], and other properties[26–28].

Over the past few years, Mustafa Lab has been repurposing various phenols and chlorophenols from out-of-use chemicals into biosafe pharmacological products, using coumarin-4-acetic acid as a lead. People stopped using the 3-(tert-butyl)-4-methoxyphenol, a food-preserving antioxidant, due to its carcinogenicity. This phenol has changed into coumarin derivatives that are safe for humans and have anti-inflammatory, anti-cancer, and anti-oxidative stress properties[29]. Additionally, two chlorophenols, 3,4-dichlorophenol and 2,3,4,5-tetrachlorophenol, have specific toxicities for humans. The former causes hormonal disturbances by inducing the estrogen receptor of the α brand, while the latter induces hepatic toxicity and teratogenicity. When these two chlorophenols were used as building blocks to make their coumarins, the compounds that were made had a lot of different biological effects, such as fighting cancer, oxidative stress, diabetes, and a wide range of microbes[30]. Finally, dinitro-ortho-cresol, a poisonous chlorophenol with broad antimicrobial activity, can lead to severe health consequences, ranging from kidney damage to death. Using coumarin-4-acetic acid as a lead, the chlorophenol underwent modification, transforming into coumarin derivatives with more potent antimicrobial potential and excellent biosafety profiles[31].

The above studies and their results led to the work that turned triclosan from a chlorophenol antimicrobial agent that wasn't needed and was bad for health into its coumarin-4-acetic acid derivative. Using various mono-, homodi-, and homotri-functionalized phenols, a $SOCl_2$-mediated esterification method created eighteen aromatic esterified coumarins from the latter. These functionalities include fluoride, chloride, nitro, nitrile, methoxy, and methyl.

Through a broth micro-diluting approach, the nineteen synthesized triclosan-based coumarins (TBCs) and three standards were studied against various pathogenic and non-pathogenic microbes. These include six aerobic bacteria, four anaerobic bacteria, two fungal strains, and three microbiome bacteria that have been approved by their ATCC codes. The studies include two branches: the antimicrobial activity tested against pathogenic microbes and biocompatibility profiling toward non-pathogenic microbes. Regarding the first study branch, the pathogenic aerobic bacterial strains employed are Pseudomonas aeruginosa (ATCC-27853, P. aeruginosa), Klebsiella pneumonia (ATCC-700603, K. pneumonia), Haemophilus influenzae (ATCC-49247, H. influenzae), Escherichia coli (ATCC-25922, E. coli), Salmonella typhi (ATCC-6539, S. typhi), and Shigella dysenteriae (ATCC-13313, S. dysenteriae). In the same branch, the utilized pathogenic anaerobic bacterial strains are Bacteroides fragilis (ATCC-25285, B. fragilis), Clostridium perfringens (ATCC-13124, C. perfringens), Fusobacterium necrophorum (ATCC-25286, F. necrophorum), and Prevotella melaninogenica (ATCC-25845, P. melaninogenica). Additionally, the study encompassed Candida albicans (ATCC-10231, C. albicans) and Aspergillus niger (ATCC-16888, A. niger). On the other hand, the second study branch that

included biocompatibility profiling used the following microbiome bacterial strains: E. coli (BAA-1427), E. coli (MG1655), and E. coli (BAA1430).

2. Materials and methods

General points. The researchers shopped in the central chemical store of the University of Mosul's College of Pharmacy for the chemicals, microbiological agents, synthesis solvents, and spectroscopical-grade solvents. According to their manufactures' instructions, the microbiological systems were ready for implementation, and we used the chemicals and solvents straight from their bottles without any additional purification. A 40 kHz, 350 W, Power Sonic-410, Korea, ultrasonic source supports a water bath in the sonication system. A single-open capillary approach using automated electrothermal apparatus (CIA-9301) was used to estimate the melting temperature ranges (mp) of the synthesized TBCs without any pre-estimation using standards. Utilizing thin-layer chromatography (TLC), the researchers were able to track the progress of the synthetic phase and ascertain the chemical purity levels. The method's stationary part was an aluminum sheet (F254) mounted with a silica gel, while the mobile section was a mixture of $CHCl_3$ and MeOH (4:1). In addition, the spectrometers used for recording the derivative spectra of ^{13}C-NMR (100 MHz) and ^{1}H-NMR (400 MHz), FTIR (400-4000 cm^{-1}), and UV-Vis (200-800 nm) were the Bruker Avance DRX-400 MHz, the Bruker-alpha-ATR-FTIR (in solid-state mode), and the UV-1600PC UV-Vis. Nevertheless, the hypothetical molecular mass (T-mass) values were calculated in Dalton unit online by means of the BMRB program (https://bmrb.io/metabolomics/mol_mass.php), whereas the Dalton-computed real molecular mass (P-mass) numbers were acquired using the Varian (7 Tesla) FTICR-MS spectrophotometer. The accuracy threshold, denoted as A-threshold and expressed in parts per million (ppm), was determined using a particular formula: (T-mass minus P-mass)/T-mass × 10^6.

Synthetic plan. The chemical synthesis, as depicted in **Scheme 1**, commences with the use of two readily available chemicals: conc. H_2SO_4 and 3-carboxy-3-hydroxypentane-1,5-dioic acid. The resulted product, 3-oxopentanedioic acid[32], was condensed with triclosan, yielding the coumarin-4-acetic acid derivative coded here as **TBC-p**. The latter was esterified individually with many functionalized phenols to produce eighteen congeners coded **TBC1-TBC18**.

Synthesis of TBC-p. Through careful warmth, a transparent ethyl acetate combination was produced from 3.5 ml of 10-mmol 3-oxyglutaric acid and 2.90 grams of 10-mmol triclosan. Using a water-ice bath to maintain a temperature under 10 °C, the resulting solution was gradually added to a 25-ml spherical beaker holding high-concentration H_2SO_4. The mixture under reaction was whisked continuously for 2.5 hours before being taken out of the ice bath and allowed to stand at room temperature overnight. On the following day, the working suspension was combined with water and crushed ice in a beaker. To obtain the desired compound, the suspended matter was collected on a filter paper, rinsed with cold water, and allowed to dry at room temperature. Recrystallizing from a 2:1 combination of benzene and methanol was used to perform the purification as a final step[33].

2-(5-Chloro-8-(2,4-dichlorophenoxy)-2-oxo-2*H*-chromen-4-yl)acetic acid (TBC-p). Pale yellow powder; yield%: 85%; mp: 210–213°C; ^{1}H-NMR (400 MHz, DMSO-d_6), ppm: 12.03 (s, 1H, carboxylic acid), 7.65–7.22 (m, 5H, aromatic protons), 7.05 (s, 1H, lactone H-3), and 4.04 (s, 2H, CH_2 of acetic acid); ^{13}C-NMR (100 MHz, DMSO-d_6), ppm: 175 (C=O, carboxylic acid), 161 (C=O coumarin), 146–112 (aromatic carbons), and 43 (CH_2, acetic acid); IR, ν_{max}, cm^{-1}: 3450–3000 (broad, O–H stretch, carboxylic acid), 1733 (C=O, acid), 1652 (C=O, coumarin), 1586 (aromatic C=C stretch), and 889 (C–Cl aromatic); ESI-MS *m/z* 401 $[M + H]^+$; calculated, %: $C_{17}H_{10}Cl_3O_5$; C: 50.04%, H: 2.47%, Cl: 31.19%, and O: 16.30%, which closely matching the expected values. These are C: 51.10%, H: 2.27%, Cl: 26.62%, and O: 20.02%.

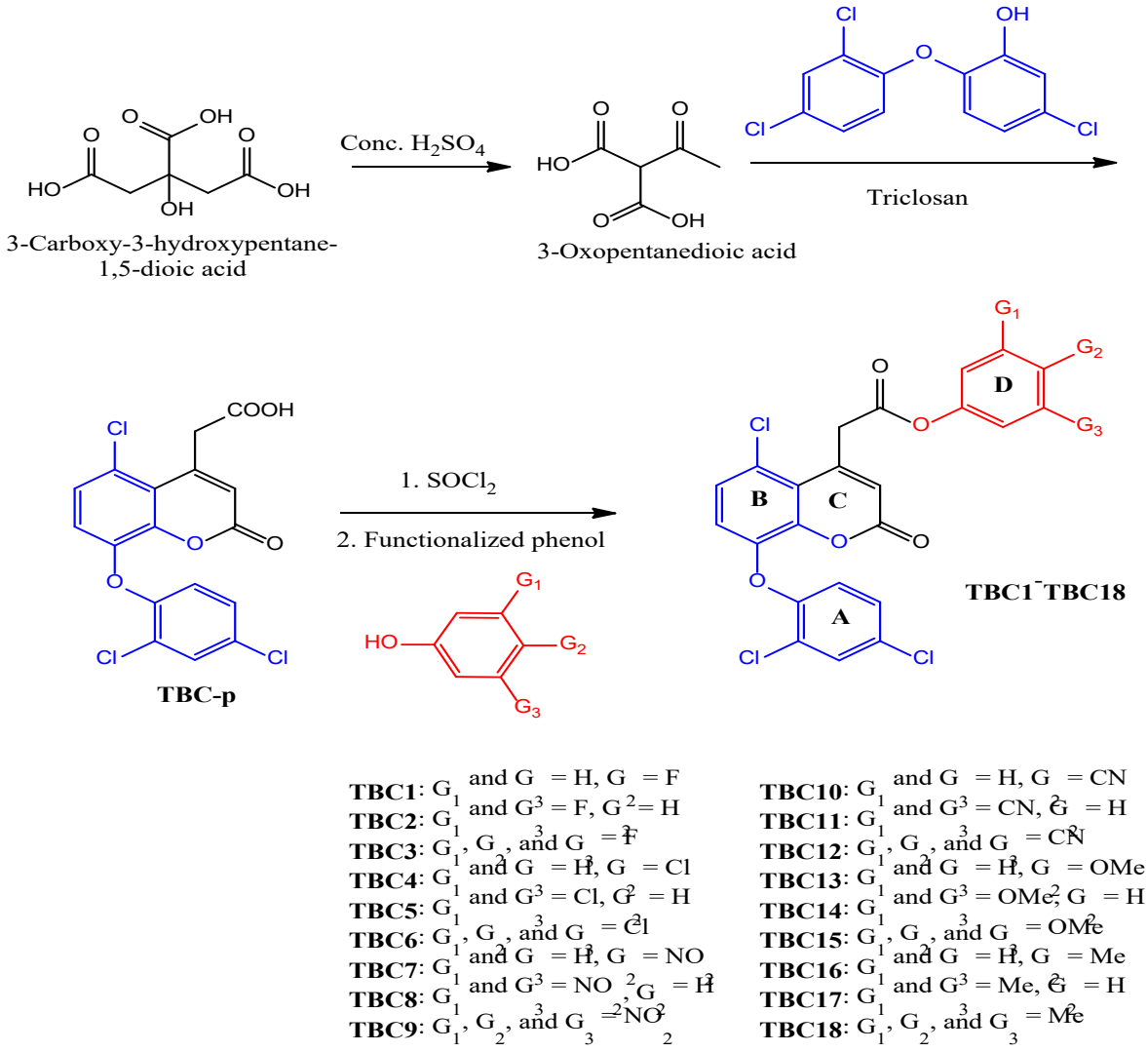

Scheme 1. The synthetic pathway yielded TBCs.

General method for synthesizing TBC1-TBC18. In a salt-ice bath, 4.0 g of 10-mmol **TBC-p** was dissolved in an excess of freshly distilled $SOCl_2$ (25 ml) under conditions of dryness. The click solution was stirred in this environment for 30 minutes and then at room temperature for the same timetable. Then, the working solution was subjected to 3-hour refluxing and removed the excess $SOCl_2$. The generated white solid representing the acyl chloride congener of **TBC-p** was treated with various 5-mmol functionalized phenols separately. Every 30-minute refluxing period, the TLC technique examined the reaction solution for product formation. As the spotting results indicated the reaction complement, the handling solution was poured into a 2-liter bucker containing a mixture of ice cube pieces and water. The immediately formed solid was cold-filtered, ice-water-washed, and left to dry. TLC checked the purity of the resultant product, and recrystallization from a specific solvent mixture established its purity[34,35].

4-Fluorophenyl 2-(5-chloro-8-(2,4-dichlorophenoxy)-2-oxo-2*H*-chromen-4-yl)acetate (TBC1). Pale yellow powder; yield%: 62%; mp: 230–233°C; ^{1}H-NMR (400 MHz, DMSO-d_6), ppm: 7.82–7.36 (m, 9H, aromatic protons), 7.12 (s, 1H, coumarin H-3), and 3.93 (s, 2H, CH_2 of the ester); ^{13}C-NMR (100 MHz, DMSO-d_6), ppm: 172 (C=O, ester), 162 (C=O coumarin), 146–112 (aromatic carbons), and 41 (CH_2, acetate group); IR, ν_{max}, cm^{-1}: 1742 (C=O, ester), 1650 (C=O, coumarin), 1582 (aromatic C=C stretch), and 889 (C–Cl aromatic); ESI-MS ***m/z* 495 [*M* + H]$^+$**; calculated, %: $C_{23}H_{14}C_{l3}FO_5$; C: 53.59%, H: 2.73%, Cl: 20.68%, F: 3.69%, and O: 19.31%, which closely matching the expected values. These are C: 55.95%, H: 2.45%, Cl: 21.54%, F: 3.85%, and O: 16.20%.

3,5-Difluorophenyl 2-(5-chloro-8-(2,4-dichlorophenoxy)-2-oxo-2*H*-chromen-4-yl)acetate (TBC2). Pale yellow powder; yield%: 55%; mp: 235–238°C; ^{1}H-NMR (400 MHz, DMSO-d_6); ppm 7.85–7.53 (m, 8H, aromatic protons), 7.20 (s, 1H, coumarin H-3), and 4.00 (s, 2H, CH_2 of the ester); ^{13}C-NMR (100 MHz, DMSO-d_6), ppm: 172 (C=O, ester), 162 (C=O coumarin), 144–116 (aromatic carbons), and 39 (CH_2, acetate group); IR, ν_{max}, cm^{-1}: 1756 (C=O, ester), 1659 (C=O, coumarin), 1585 (aromatic C=C stretch), and 889 (C–Cl aromatic); ESI-MS ***m/z* 512 [*M* + H]$^+$;** calculated, %: $C_{23}H_{13}Cl_3F_2O_5$; C: 51.81%, H: 2.46%, Cl: 19.94%, F: 7.09%, and O: 18.70%, closely matching the expected values. These are C: 53.99%, H: 2.17%, Cl: 20.79%, F: 7.43%, and O: 15.63%.

3,4,5-Trifluorophenyl 2-(5-chloro-8-(2,4-dichlorophenoxy)-2-oxo-2*H*-chromen-4-yl)acetate (TBC3). Pale yellow powder; yield%: 49%; mp: 240–243°C; ^{1}H-NMR (400 MHz, DMSO-d_6), ppm: 7.80–7.38 (m, 7H, aromatic protons), 7.24 (s, 1H, coumarin H-3), and 4.07 (s, 2H, CH_2 of the ester); ^{13}C-NMR (100 MHz, DMSO-d_6), ppm: 171 (C=O, ester), 162 (C=O coumarin), 141–112 (aromatic carbons), and 42 (CH_2, acetate group); IR, ν_{max}, cm^{-1}: 1757 (C=O, ester), 1659 (C=O, coumarin), 1585 (aromatic C=C stretch), and 889 (C–Cl aromatic); ESI-MS *m/z* 531 [*M* + H]$^+$; calculated, %: $C_{23}H_{12}Cl_3F_3O_5$; C: 50.11%, H: 2.20%, Cl: 19.27%, F: 10.34%, and O: 18.08%, closely matching the expected values. These are C: 52.15%, H: 1.90%, Cl: 20.08%, F: 10.76%, and O: 15.10%.

4-Chlorophenyl 2-(5-chloro-8-(2,4-dichlorophenoxy)-2-oxo-2*H*-chromen-4-yl)acetate (TBC4). Pale yellow powder; yield%: 65%; mp: 225–228°C; ^{1}H-NMR (400 MHz, DMSO-d_6); ppm: 7.77–7.43 (m, 9H, aromatic protons), 7.18 (s, 1H, coumarin H-3), and 3.98 (s, 2H, CH_2 of the ester); ^{13}C-NMR (100 MHz, DMSO-d_6); ppm: 172 (C=O, ester), 161 (C=O coumarin), 142–113 (aromatic carbons), and 41 (CH_2, acetate group); IR, ν_{max}, cm^{-1}: 1751 (C=O, ester), 1667 (C=O, coumarin), 1585 (aromatic C=C stretch), and 888 (C–Cl aromatic); ESI-MS *m/z* **511 [*M* + H]$^+$;** calculated, %: $C_{23}H_{13}Cl_4O_5$; C: 51.73%, H: 2.45%, Cl: 26.57%, and O: 19.25%, closely matching the expected values. These are C: 54.15%, H: 2.37%, Cl: 27.80%, and O: 15.68%.

3,5-Dichlorophenyl 2-(5-chloro-8-(2,4-dichlorophenoxy)-2-oxo-2*H*-chromen-4-yl)acetate (TBC5). Pale yellow powder; yield%: 62%; mp: 230–235°C; ^{1}H-NMR (400 MHz, DMSO-d_6), ppm: 7.81–7.36 (m, 8H, aromatic protons), 7.22 (s, 1H, coumarin H-3), and 4.01 (s, 2H, CH_2 of the ester); ^{13}C-NMR (100 MHz, DMSO-d_6), ppm: 172 (C=O, ester), 162 (C=O coumarin), 141–113 (aromatic carbons), and 38 (CH_2, acetate group); IR, ν_{max}, cm^{-1}: 1756 (C=O, ester), 1659 (C=O, coumarin), 1585 (aromatic C=C stretch), and (C–Cl aromatic); ESI-MS *m/z* 546 [*M* + H]$^+$; calculated, %: $C_{23}H_{12}Cl_5O_5$; C: 48.18%, H: 2.11%, Cl: 35.68%, and O: 14.03%, closely matching the expected values. These are C: 50.73%, H: 2.04%, Cl: 32.55%, and O: 14.69%.

3,4,5-Trichlorophenyl 2-(5-chloro-8-(2,4-dichlorophenoxy)-2-oxo-2*H*-chromen-4-yl)acetate (TBC6). Pale yellow powder; yield%: 56%; mp: 235–240°C; ^{1}H-NMR (400 MHz, DMSO-d_6), ppm: 7.82–7.38 (m, 7H, aromatic protons), 7.24 (s, 1H, coumarin H-3), and 4.03 (s, 2H, CH_2 of the ester); ^{13}C-NMR (100 MHz, DMSO-d_6); ppm: 172 (C=O, ester), 161 (C=O coumarin), 141–112 (aromatic carbons), and 41 (CH_2, acetate group); IR, ν_{max}, cm^{-1}: 1761 (C=O, ester), 1658 (C=O, coumarin), 1587 (aromatic C=C stretch), and 888 (C–Cl aromatic); ESI-MS *m/z* **580 [*M* + H]$^+$**; calculated, %: $C_{23}H_{11}Cl_6O_5$; C: 44.90%, H: 1.80%, Cl: 40.95%, and O: 12.35%, closely matching the expected values. These are C: 47.71%, H: 1.74%, Cl: 36.74%, and O: 13.82%.

4-Nitrophenyl 2-(5-chloro-8-(2,4-dichlorophenoxy)-2-oxo-2*H*-chromen-4-yl)acetate (TBC7). Pale yellow powder; yield%: 44%; mp: 210–215°C; ^{1}H-NMR (400 MHz, DMSO-d_6), ppm: 7.84–7.36 (m, 9H, aromatic protons), 7.22 (s, 1H, coumarin H-3), and 4.03 (s, 2H, CH_2 of the ester); ^{13}C-NMR (100 MHz, DMSO-d_6), ppm: 172 (C=O, ester), 162 (C=O coumarin), 142.0–118 (aromatic carbons), and 40 (CH_2, acetate group); IR, ν_{max}, cm^{-1}: 1758 (C=O, ester), 1656 (C=O, coumarin), 1588 (aromatic C=C stretch), 1522 and 1353 (NO_2 symmetric and asymmetric stretches), and 885 (C–Cl aromatic); ESI-MS *m/z* **521 [*M* + H]$^+$;** calculated, %:

$C_{23}H_{12}Cl_3NO_7$; C: 52.86%, H: 2.31%, Cl: 20.34%, N: 2.68%, and O: 21.81%, closely matching the expected values. These are C: 53.05%, H: 2.32%, Cl: 20.43%, N: 2.69%, and O: 21.51%.

3,5-Dinitrophenyl 2-(5-chloro-8-(2,4-dichlorophenoxy)-2-oxo-2*H*-chromen-4-yl)acetate (TBC8). Pale yellow powder; yield%: 42%; mp: 220–225°C; ^{1}H-NMR (400 MHz, DMSO-d_6), ppm: 7.85–7.34 (m, 8H, aromatic protons), 7.22 (s, 1H, coumarin H-3), and 4.02 (s, 2H, CH_2 of the ester); ^{13}C-NMR (100 MHz, DMSO-d_6), ppm: 172 (C=O, ester), 161 (C=O coumarin), 142–118 (aromatic carbons), and 41 (CH_2, acetate group); IR, ν_{max}, cm^{-1}: 1756 (C=O, ester), 1658 (C=O, coumarin), 1587 (aromatic C=C stretch), 1540 and 1340 (NO_2 symmetric and asymmetric stretches), and 886 (C–Cl aromatic); ESI-MS *m/z* **567 [*M* + H]$^+$;** calculated, %: $C_{23}H_{11}Cl_3N_2O_9$; C: 48.68%, H: 1.95%, Cl: 18.73%, N: 4.93%, and O: 25.71%, closely matching the expected values. These are C: 48.83%, H: 1.96%, Cl: 18.80%, N: 4.95%, and O: 25.45%.

3,4,5-Trinitrophenyl 2-(5-chloro-8-(2,4-dichlorophenoxy)-2-oxo-2*H*-chromen-4-yl)acetate (TBC9). Pale yellow powder; yield%: 42%; mp: 230–235°C; ^{1}H-NMR (400 MHz, DMSO-d_6), ppm: 7.82–7.38 (m, 7H, aromatic protons), 7.24 (s, 1H, coumarin H-3), and 4.01 (s, 2H, CH_2 of the ester); ^{13}C-NMR (100 MHz, DMSO-d_6), ppm: 172 (C=O, ester), 162 (C=O coumarin), 142–116 (aromatic carbons including trinitrophenyl carbons), and 42 (CH_2, acetate group); IR, ν_{max}, cm^{-1}: 1754 (C=O, ester), 1654 (C=O, coumarin), 1586 (aromatic C=C stretch), 1553 and 1341 (NO_2 symmetric and asymmetric stretches), and 884 (C–Cl aromatic); ESI-MS *m/z* **612 [*M* + H]$^+$;** calculated, %: $C_{23}H_{10}Cl_3N_3O_{11}$; C: 45.13%, H: 1.65%, Cl: 17.43%, N: 6.86%, and O: 28.93%, closely matching the expected values. These are C: 45.23%, H: 1.65%, Cl: 17.42%, N: 6.88%, and O: 28.82%.

4-Cyanophenyl 2-(5-chloro-8-(2,4-dichlorophenoxy)-2-oxo-2*H*-chromen-4-yl)acetate (TBC10). Pale yellow powder; yield%: 63%; mp: 220–225°C; ^{1}H-NMR (400 MHz, DMSO-d_6), ppm: 7.83–7.38 (m, 9H, aromatic protons), 7.26 (s, 1H, coumarin H-3), and 4.01 (s, 2H, CH_2 of the ester); ^{13}C-NMR (100 MHz, DMSO-d_6), ppm: 172 (C=O, ester), 160 (C=O coumarin), 148–116 (aromatic carbons including cyano-substituted carbons), 118 (C≡N), and 38 (CH_2, acetate group); IR, ν_{max}, cm^{-1}: 1761 (C=O, ester), 1659 (C=O, coumarin), 1588 (aromatic C=C stretch), 2223 (C≡N stretch), and 885 (C–Cl aromatic); ESI-MS *m/z* **502 [*M* + H]$^+$;** calculated, %: $C_{24}H_{12}Cl_3NO_5$; C: 55.42%, H: 2.32%, Cl: 20.51%, N: 2.70%, and O: 18.05%, closely matching the expected values. These are C: 57.57%, H: 2.42%, Cl: 21.24%, N: 2.80%, and O: 15.98%.

3,5-Dicyanophenyl 2-(5-chloro-8-(2,4-dichlorophenoxy)-2-oxo-2*H*-chromen-4-yl)acetate (TBC11). Pale yellow powder; yield%: 60%; mp: 225–230°C; ^{1}H-NMR (400 MHz, DMSO-d_6), ppm: 7.82–7.38 (m, 8H, aromatic protons), 7.22 (s, 1H, coumarin H-3), and 4.04 (s, 2H, CH_2 of the ester); ^{13}C-NMR (100 MHz, DMSO-d_6), ppm: 172 (C=O, ester), 161 (C=O coumarin), 142–116 (aromatic carbons including cyano-substituted carbons), 114 (C≡N), and 39 (CH_2, acetate group); IR, ν_{max}, cm^{-1}: 1762 (C=O, ester), 1656 (C=O, coumarin), 1586 (aromatic C=C stretch), 2224 (C≡N stretch), and 882 (C–Cl aromatic); ESI-MS *m/z* **527 [*M* + H]$^+$;** calculated, %: $C_{25}H_{11}Cl_3N_2O_5$; C: 55.03%, H: 2.03%, Cl: 19.51%, N: 5.13%, and O: 18.30%, closely matching the expected values. These are C: 57.12%, H: 2.11%, Cl: 20.23%, N: 5.33%, and O: 15.22%.

3,4,5-Tricyanophenyl 2-(5-chloro-8-(2,4-dichlorophenoxy)-2-oxo-2*H*-chromen-4-yl)acetate (TBC12). Pale yellow powder; yield%: 55%; mp: 230–235°C; ^{1}H-NMR (400 MHz, DMSO-d_6), ppm: 7.85–7.38 (m, 8H, aromatic protons), 7.22 (s, 1H, coumarin H-3), and 38 (s, 2H, CH_2 of the ester); ^{13}C-NMR (100 MHz, DMSO-d_6), ppm: 172 (C=O, ester), 162 (C=O coumarin), 144–118 (aromatic carbons including cyano-substituted carbons), 115 (C≡N), and 40 (CH_2, acetate group); IR, ν_{max}, cm^{-1}: 1758 (C=O, ester), 1656 (C=O, coumarin), 1586 (aromatic C=C stretch), 2224 (C≡N stretch), and 883 (C–Cl aromatic); ESI-MS *m/z* **552 [*M* + H]$^+$**; calculated, %: $C_{26}H_{10}Cl_3N_3O_5$; C: 53.68%, H: 1.74%, Cl: 18.53%, N: 7.23%, and O: 19.82%, closely matching the expected values. These are C: 56.70%, H: 1.83%, Cl: 19.31%, N: 7.63%, and O: 14.53%.

4-Methoxyphenyl 2-(5-chloro-8-(2,4-dichlorophenoxy)-2-oxo-2*H*-chromen-4-yl)acetate (TBC13). Pale yellow powder; yield%: 80%; mp: 210–215°C; ^{1}H-NMR (400 MHz, DMSO-d_6), ppm: 7.82–7.38 (m, 9H, aromatic protons), 7.21 (s, 1H, coumarin H-3), 4.01 (s, 2H, CH_2 of the ester), and 3.72 (s, 3H, methoxy group);

^{13}C-NMR (100 MHz, DMSO-*d*$_6$), ppm: 172 (C=O, ester), 161 (C=O coumarin), 142–112 (aromatic carbons including methoxyphenyl and coumarin carbons), 56 (OCH_3), and 38 (CH_2, acetate group); IR, ν_{max}, cm^{-1}: 2855 (C–H stretch from methoxy), 1762 (C=O, ester), 1662 (C=O, coumarin), 1588 (aromatic C=C stretch), and 884 (C–Cl aromatic); ESI-MS *m/z* **507 [*M* + H]$^+$;** calculated, %: $C_{24}H_{14}Cl_3O_5$; C: 56.91%, H: 2.79%, Cl: 19.86%, and O: 20.44%, closely matching the expected values. These are C: 57.00%, H: 2.99%, Cl: 21.03%, and O: 18.98%.

3,5-Dimethoxyphenyl 2-(5-chloro-8-(2,4-dichlorophenoxy)-2-oxo-2*H*-chromen-4-yl)acetate (TBC14). Pale yellow powder; yield%: 84%; mp: 215–220°C; ^{1}H-NMR (400 MHz, DMSO-*d*$_6$), ppm: 7.83–7.38 (m, 8H, aromatic protons), 7.22 (s, 1H, coumarin H-3), 4.01 (s, 2H, CH_2 of the ester), and 3.74 (s, 6H, methoxy groups); ^{13}C-NMR (100 MHz, DMSO-*d*$_6$), ppm: 171 (C=O, ester), 160 (C=O coumarin), 144–116 (aromatic carbons), 58 (OCH_3), and 39 (CH_2, acetate group); IR, ν_{max}, cm^{-1}: 2866 (C–H stretch from methoxy), 1762 (C=O, ester), 1658 (C=O, coumarin), 1588 (aromatic C=C stretch), and 885 (C–Cl aromatic); ESI-MS *m/z* **537 [*M* + H]$^+$;** calculated, %: $C_{25}H_{16}Cl_3O_6$; C: 57.32%, H: 3.06%, Cl: 19.12%, and O: 20.50%, closely matching the expected values. These are C: 56.05%, H: 3.20%, Cl: 19.85%, and O: 20.90%.

3,4,5-Trimethoxyphenyl 2-(5-chloro-8-(2,4-dichlorophenoxy)-2-oxo-2*H*-chromen-4-yl)acetate (TBC15). Pale yellow powder; yield%: 89%; mp: 220–225°C; ^{1}H-NMR (400 MHz, DMSO-*d*$_6$), ppm: 7.84–7.38 (m, 7H, aromatic protons), 7.26 (s, 1H, coumarin H-3), 4.02 (s, 2H, CH_2 of the ester), and 3.76 (s, 9H, methoxy groups); ^{13}C-NMR (100 MHz, DMSO-*d*$_6$), ppm: 171 (C=O, ester), 163 (C=O coumarin), 143–115 (aromatic carbons), 58 (OCH_3), and 42 (CH_2, acetate group); IR, ν_{max}, cm^{-1}: 2858 (C–H stretch from methoxy), 1758 (C=O, ester), 1656 (C=O, coumarin), 1587 (aromatic C=C stretch), and 888 (C–Cl aromatic); ESI-MS *m/z* **567 [*M* + H]$^+$;** calculated, %: $C_{26}H_{18}Cl_3O_7$; C: 58.27%, H: 3.17%, Cl: 18.50%, and O: 20.06%, closely matching the expected values. These are C: 55.19%, H: 3.38%, Cl: 18.80%, and O: 22.62%.

***p*-Tolyl 2-(5-chloro-8-(2,4-dichlorophenoxy)-2-oxo-2*H*-chromen-4-yl)acetate (TBC16)**. Pale yellow powder; yield%: 81%; mp: 215–220°C; ^{1}H-NMR (400 MHz, DMSO-*d*$_6$), ppm: 7.82–7.38 (m, 9H, aromatic protons), 7.24 (s, 1H, coumarin H-3), 4.01 (s, 2H, CH_2 of the ester), and 2.46 (s, 3H, methyl group); ^{13}C-NMR (100 MHz, DMSO-*d*$_6$), ppm: 171 (C=O, ester), 163 (C=O coumarin), 1454–116 (aromatic carbons), 41 (CH_2, acetate group), and 22 (methyl group); IR, ν_{max}, cm^{-1}: 2865 (C–H stretch from the methyl group), 1762 (C=O, ester), 1658 (C=O, coumarin), 1586 (aromatic C=C stretch), and 884 (C–Cl aromatic); ESI-MS *m/z* **491 [M + H]$^+$;** calculated, %: $C_{23}H_{15}Cl_3O_4$; C: 60.87%, H: 3.33%, Cl: 17.84%, and O: 17.96%, closely matching the expected values. These are C: 58.86%, H: 3.09%, Cl: 21.72%, and O: 16.33%.

3,5-Dimethylphenyl 2-(5-chloro-8-(2,4-dichlorophenoxy)-2-oxo-2*H*-chromen-4-yl)acetate (TBC17). Pale yellow powder; yield%: 84%; mp: 210–215°C; ^{1}H-NMR (400 MHz, DMSO-*d*$_6$), ppm: 7.82–7.38 (m, 8H, aromatic protons), 7.27 (s, 1H, coumarin H-3), 4.00 (s, 2H, CH_2 of the ester), and 2.18 (s, 6H, methyl groups); ^{13}C-NMR (100 MHz, DMSO-*d*$_6$), ppm: 171 (C=O, ester), 163 (C=O coumarin), 144–114 (aromatic carbons), 42 (CH_2, acetate group), and 23 (methyl groups); IR, ν_{max}, cm^{-1}: 2868 (C–H stretch from methyl groups), 1762 (C=O, ester), 1658 (C=O, coumarin), 1588 (aromatic C=C stretch), and 882 (C–Cl aromatic); ESI-MS *m/z* **505 [*M* + H]$^+$;** calculated, %: $C_{23}H_{17}Cl_3O_4$; C: 61.67%, H: 4.13%, Cl: 18.46%, and O: 17.74%, closely matching the expected values. These are C: 59.61%, H: 3.40%, Cl: 21.11%, and O: 15.88%.

3,4,5-Trimethylphenyl 2-(5-chloro-8-(2,4-dichlorophenoxy)-2-oxo-2*H*-chromen-4-yl)acetate (TBC18). Pale yellow powder; yield%: 87%; mp: 215–220°C; ^{1}H-NMR (400 MHz, DMSO-*d*$_6$), ppm: 7.82–7.38 (m, 7H, aromatic protons), 7.26 (s, 1H, coumarin H-3), 4.04 (s, 2H, CH_2 of the ester), and 2.36 (s, 9H, methyl groups); ^{13}C-NMR (100 MHz, DMSO-*d*$_6$), ppm: 174 (C=O, ester), 160 (C=O coumarin), 148–116 (aromatic carbons), 40 (CH_2, acetate group), and 23 (methyl groups); IR, ν_{max}, cm^{-1}: 1758 (C=O, ester), 1658 (C=O, coumarin), 1586 (aromatic C=C stretch), 2868 (C–H stretch from methyl groups), and 882 (C–Cl

aromatic); ESI-MS *m/z* **519 [*M* + H]$^+$;** calculated, %: $C_{24}H_{18}Cl_3O_4$; C: 60.09%, H: 3.78%, Cl: 18.95%, and O: 17.89%, closely matching the expected values. These are C: 60.31%, H: 3.70%, Cl: 20.54%, and O: 15.45%.

Evaluating the activity against pathogenic aerobic bacteria. This activity of the test compounds against pathogenic aerobic bacteria was assessed using the broth microdilution method. Mueller-Hinton broth (MHB) was employed as the growth medium, with ciprofloxacin (CIP) serving as the positive control and dimethyl sulfoxide (DMSO) as the negative control. A stock solution was prepared by dissolving 1 mg of each test compound in 1 ml of DMSO and then serially diluted twofold with sterilized water to obtain 12 solutions with concentrations ranging from 1024 to 0.25 µg/ml. For each test, 3 ml of MHB, 2 ml of inoculum (adjusted to 0.5 McFarland standard), and 1 ml of the respective concentration of the test solution were combined in labeled test tubes. The prepared mixtures were incubated at 37 °C for 24 hours, and the minimum inhibitory concentration (MIC) was determined as the lowest concentration that completely inhibited bacterial growth[36].

To determine the minimum bactericidal concentration (MBC), the concentration immediately above the MIC in the serial dilution sequence was further aqueous-diluted to final concentrations on the basis of adding 0.05, 0.5, 1, or 4 concentration factors to that of the MIC. The MIC-determined protocol was repeated with these dilutions to assess the second microbiological measure, MBC[37]. The potency marker (PM) represents the third detected microbiological measure that was calculated by dividing the MBC value by the corresponding MIC value. Based on the PM, the mode of activity was categorized: a PM value greater than 4 indicated bacteriostatic activity, while a PM value of 4 or less indicated bactericidal activity[38].

Evaluating the other microbiological activities. The baseline protocol for assessing antibacterial activity against pathogenic aerobic bacteria was adapted to evaluate other microbiological activities of the test chemicals. For activity against pathogenic anaerobic bacteria, modifications were made to the standard protocol. The growth medium was replaced with Brucella agar supplemented with 5% sheep blood, and metronidazole (MET) was used as the positive control. Also, the incubation process was extended to 48 hours and conducted in an anaerobic jar. The latter was maintained in an oxygen-free environment using an anaerobic gas generation system, an anaerobe indicator, and palladium as a catalyst to ensure proper anaerobic conditions [39]. Given the antifungal activity, the baseline protocol was modified by replacing the growth medium with Sabouraud-dextrose broth and the positive control with nystatin (NYT). Additionally, the incubation process was adjusted to 48 hours at 30 °C to accommodate fungal growth requirements[40]. Finally, to assess the biocompatibility of the test chemicals with microbiome bacteria, the baseline protocol was applied without any modifications[41].

3. Results and discussion

3.1. Chemistry

The synthesis of precursor **TBC-p** and its aromatic-esterified derivatives (**TBC1**-**TBC18**) was performed through sequential steps. In the first one, 3-oxopentanedioic acid was prepared through a previously published paper by condensing 3-carboxy-3-hydroxypentane-1,5-dioic acid with conc. H_2SO_4 via a decarboxylation-mediated mechanism[42]. Because of the strong concentration of inorganic acid used, it is impossible to follow up on the reaction progress via the TLC technique. Therefore, the stoppage of bubble release represents the best visible indicator of the reaction complement[43].

In the second synthetic step, the application of the Pechmann condensation reaction created the precursor **TBC-p**. The process involves the condensation of 3-oxopentanedioic acid with triclosan in the presence of concentrated H_2SO_4, which serves as both a catalyst and a drying agent [44]. The researchers utilized an excess amount of the acid as a reaction medium to fulfill these two roles, resulting in a comparatively high yield of 85.13%[45]. Since the progress of this synthetic reaction can't be detected via the TLC technique, as in the first step, long room temperature-performed mixing was applied (18 hours)[46]. The elemental and spectroscopic

examinations confirm the formation of **TBC-p**. The latter examination clearly reveals the presence of a carboxylic acid moiety in the FTIR and ^{1}H-NMR charts[47].

$SOCl_2$-catalyzed esterification of **TBC-p** with various phenols was the final synthetic step. The number and type of substitutions distinguish these phenols from one another. Given the latter factor, the substitution types used included fluoride, chloride, nitro, cyano, methoxy, and methyl entities. Regarding the substitution number, it was one, two, or three[48]. The spectroscopic methods were utilized to identify the esterified compounds (**TBC1**–**TBC18**) by observing the disappearance of the carboxylic acid moiety and the appearance of an aliphatic ester motif[49]. One of the most notable aspects of this synthetic step is the significant variation in the yield% values, ranging from 86.52 to 41.56%. The researchers concluded by analyzing this variation that the yield percentage directly relates to the number and capacity of the original phenolic substitution to donate electrons[50]. Accordingly, **TBC15**, which constructs from a phenol-trisubstituted with methoxy groups, has the highest yield% value. The other conclusion is that the relationship is reversed when considering those with electron-withdrawing functionality[51]. Therefore, **TBC9**, a phenol-trisubstituted compound with nitro groups, correlates with the lowest yield% value.

3.2. Microbiology

3.2.1. Antibacterial activity against pathogenic aerobes

Aerobic bacterial pathogens are an increasing threat to health because they can cause a broad variety of ailments, from minor skin infections to serious system-wide illnesses[52]. These bacteria flourish in surroundings high in oxygen. Common aerobic bacteria like E. coli and P. aeruginosa can cause infections of the urinary system, respiratory tract, wounds, and sepsis[53]. Because they can thrive in environments with weak immune systems and create biofilms on medical equipment, these bacteria pose a serious threat to patients in healthcare facilities, where they can develop resistance to antibiotics[54]. The emergence of multidrug-resistant strains of aerobic bacteria has further compounded the problem, decreasing remedies and increasing the likelihood of complications like longer hospital stays, more medical bills, and even death[55]. Strict infection control protocols, cutting-edge diagnostic equipment, and unceasing investigation into potential antibiotic and non-antibiotic treatment options are necessary to combat infections caused by this bacterial type[56–58].

We used the broth microdilution methodology to score our TBCs' ability to inhibit the pathogenic growth of six aerobic bacterial strains by calculating three measures: MIC, MBC, and PM[59]. For the first one, **Table 1** shows that the MIC values in μg/ml for the CIP, the precursor **TBC-p**, and the esterified coumarins (**TBC1**–**TBC18**) are 0.70–1.60, 10.85–13.20, and 1.10–6.95, respectively. Additionally, the synthesized TBCs showed less activity compared to CIP, albeit to varying degrees. In comparison to its esterified congeners, **TBC-p** demonstrated significantly less activity. This fact underscores the significance of aromatic esterification of the precursor carboxylic acid, as it possesses a high hydrophilic character that could potentially restrict the compound's penetration into aerobic bacteria[60]. For the esterified coumarins, we found that the activity depends on the substitution map located on ring D. In more detail, we found that the coumarins with one substitution on this ring are less active than those with two, and those with two are less active than those with three[61]. Another important factor is the type of substituted moiety, which arranges the order of activity in a descending order: chloride, fluoride, methoxy, methyl, cyano, and nitro[62]. Based on these outcomes, **TBC6**, which has three chloride moieties on ring D, is the compound with the highest activity among all the synthesized compounds. In the literature, we find that the presence of an aromatic chloride framework can enhance the antibacterial activity against pathogenic aerobes. This fact aligns with our final conclusion[63–66].

Table 1. The MIC values of the CIP as well as **TBC-p** and its esterified coumarins against pathogenic aerobes.

Bacterial strain	Codes of the positive control and TBCs									
	CIP	**TBC-p**	**TBC1**	**TBC2**	**TBC3**	**TBC4**	**TBC5**	**TBC6**	**TBC7**	**TBC8**
P. aeruginosa	1.05	11.15	2.30	2.25	2.10	1.70	1.65	1.55	6.30	6.25
K. pneumonia	0.70	10.85	2.15	2.10	1.95	1.55	1.35	1.15	6.45	6.40
H. influenzae	1.15	11.40	2.55	2.40	2.25	2.05	1.95	1.80	6.15	6.10
E. coli	1.25	11.75	2.45	2.40	2.35	1.90	1.80	1.65	6.95	6.80
S. typhi	1.60	12.05	2.95	2.85	2.50	1.90	1.85	1.80	6.95	6.90
S. dysenteriae	0.95	13.20	2.55	2.30	2.05	1.40	1.25	1.10	6.35	6.20
Bacterial strain	**Codes of the TBCs**									
	TBC9	**TBC10**	**TBC11**	**TBC12**	**TBC13**	**TBC14**	**TBC15**	**TBC16**	**TBC17**	**TBC18**
P. aeruginosa	6.10	4.75	4.60	4.45	2.75	2.55	2.35	3.40	3.25	3.10
K. pneumonia	6.25	4.90	4.85	4.85	2.45	2.35	2.30	3.65	3.20	3.05
H. influenzae	6.15	4.75	4.70	4.60	2.90	2.75	2.70	3.55	3.30	3.30
E. coli	6.95	5.10	5.15	4.95	2.75	2.65	2.50	3.65	3.40	3.15
S. typhi	6.80	5.05	4.90	4.75	3.15	3.10	3.15	3.70	3.55	3.40
S. dysenteriae	6.05	4.45	4.35	4.30	2.65	2.60	2.55	3.25	3.25	3.20

The µg/ml is the unit used to define the MIC values

The second computed microbiological measure, MBC, represents the concentration of the chemical that can kill the exposed bacteria. So, it is logical to be greater than that of MIC[67]. **Table 2** presents the numerical values used to calculate the MBC for the CIP, along with the **TBC-p** and its esterified coumarins against the studied aerobic bacteria. Analyzing these values reveals a parallel relationship with the MIC values, using the same rationale. Given the numbers found in **Table 3**, which are less than 4, the synthesized compounds collectively act as bactericidal rather than bacteriostatic against the pathogenic aerobes under study[68–70].

Table 2. The MBC values of the CIP as well as **TBC-p** and its esterified coumarins against pathogenic aerobes.

Bacterial strain	Codes of the positive control and TBCs									
	CIP	**TBC-p**	**TBC1**	**TBC2**	**TBC3**	**TBC4**	**TBC5**	**TBC6**	**TBC7**	**TBC8**
P. aeruginosa	2.00	22.15	3.05	3.25	2.55	2.80	2.00	1.70	11.90	10.40
K. pneumonia	1.30	21.55	2.85	3.05	2.35	2.55	1.65	1.30	12.20	10.65
H. influenzae	2.15	22.65	3.40	3.45	2.75	3.40	2.40	2.00	11.60	10.15
E. coli	2.35	23.35	3.25	3.45	2.85	3.15	2.20	1.85	13.15	11.35
S. typhi	3.00	23.95	3.95	4.10	3.05	3.15	2.25	2.00	13.10	11.50
S. dysenteriae	1.80	26.25	3.40	3.30	2.50	2.30	1.55	1.20	12.00	10.35
Bacterial strain	**Codes of the TBCs**									
	TBC9	**TBC10**	**TBC11**	**TBC12**	**TBC13**	**TBC14**	**TBC15**	**TBC16**	**TBC17**	**TBC18**
P. aeruginosa	8.15	6.34	6.15	5.95	3.65	3.40	3.15	4.55	4.35	4.15
K. pneumonia	8.35	6.54	6.50	6.45	3.25	3.15	3.10	4.90	4.30	4.10
H. influenzae	8.20	6.34	6.30	6.15	3.85	3.65	3.60	4.75	4.40	4.40
E. coli	9.30	6.81	6.95	6.60	3.65	3.55	3.35	4.85	4.55	4.20
S. typhi	9.10	6.74	6.55	6.35	4.20	4.15	4.20	4.90	4.75	4.55
S. dysenteriae	8.10	5.94	5.80	5.75	3.55	3.50	3.40	4.35	4.35	4.30

The µg/ml is the unit used to define the MBC values

Table 3. The PM values of the CIP as well as **TBC-p** and its esterified coumarins against pathogenic aerobes.

Bacterial strain	Codes of the positive control and TBCs									
	CIP	**TBC-p**	**TBC1**	**TBC2**	**TBC3**	**TBC4**	**TBC5**	**TBC6**	**TBC7**	**TBC8**
P. aeruginosa	1.905	1.987	1.326	1.444	1.214	1.647	1.212	1.097	1.889	1.664
K. pneumonia	1.857	1.986	1.326	1.452	1.205	1.645	1.222	1.130	1.891	1.664
H. influenzae	1.870	1.987	1.333	1.438	1.222	1.659	1.231	1.111	1.886	1.664
E. coli	1.880	1.987	1.327	1.438	1.213	1.658	1.222	1.121	1.892	1.669
S. typhi	1.875	1.988	1.339	1.439	1.220	1.658	1.216	1.111	1.885	1.667
S. dysenteriae	1.895	1.989	1.333	1.435	1.220	1.643	1.240	1.091	1.890	1.669
Bacterial strain	Codes of the TBCs									
	TBC9	**TBC10**	**TBC11**	**TBC12**	**TBC13**	**TBC14**	**TBC15**	**TBC16**	**TBC17**	**TBC18**
P. aeruginosa	1.336	1.336	1.337	1.337	1.327	1.333	1.340	1.338	1.338	1.339
K. pneumonia	1.336	1.336	1.340	1.330	1.327	1.340	1.348	1.342	1.344	1.344
H. influenzae	1.333	1.336	1.340	1.337	1.328	1.327	1.333	1.338	1.333	1.333
E. coli	1.338	1.336	1.350	1.333	1.327	1.340	1.340	1.329	1.338	1.333
S. typhi	1.338	1.336	1.337	1.337	1.333	1.339	1.333	1.324	1.338	1.338
S. dysenteriae	1.339	1.336	1.333	1.337	1.340	1.346	1.333	1.338	1.338	1.344

3.3. Antibacterial activity against pathogenic anaerobes

Pathogenic anaerobic bacteria, which can survive in low-oxygen environments such as deep tissues, wounds, or internal organs, are a major cause for concern when it comes to infections[71].These infections often accompany illnesses that affect the gums, teeth, blood vessels, intestines, or pelvis[72]. Anaerobic bacteria, like those in the genus *Fusobacterium*, genus *Clostridium*, and other similar species, make toxins and enzymes that hurt host tissues, make inflammation worse, and weaken immune responses[73]. Untreated infections can lead to severe issues like tissue necrosis, systemic inflammation, organ failure, and even apoptosis[74]. For successful handling of these infections and reducing the probability of long-term health repercussions, timely detection and tailored treatment are critical. Often, the latter factor involves antibacterial drugs like metronidazole or clindamycin[75].

With antibiotic resistance on the rise among anaerobic pathogens, it is crucial to find novel anti-anaerobic bacterial options[76]. That being said, a large number of these bacteria have evolved resistance to widely used antibiotics, which increases the likelihood of treatment failure and narrows the choices for curative measures[77]. Also, ordinary antibiotics have a difficult time killing anaerobes because of their unusual physiology. Not only is it critical to find novel therapeutic agents to combat resistance, but it is also critical to develop biocompatible, more effective medicines with fewer adverse effects[78]. Novel classes of antibiotics, antimicrobial peptides, and targeted treatments are examples of creativity that have the potential to dramatically boost clinical results for these challenging infections[79].

Using the broth microdilution method, we tested our TBCs to see if they could stop the growth of four harmful anaerobic bacterial strains in their ideal conditions. During this evaluation, we calculated three parameters: MIC, MBC, and PM. The MIC values for the MET, the precursor **TBC-p**, and the esterified coumarins are 0.95-2.85, 47.20-45.45, and 4.35-7.85, respectively, according to **Table 4**. The amount to which synthesized TBCs were less active than MET varied. Notably, **TBC-p** exhibited far lower activity compared to its esterified counterparts. This overstates the importance of the aromatic esterification of the carboxylic acid precursor, as its hydrophilic nature may limit the compound's ability to penetrate anaerobic bacteria. Also,

we observed that the esterified coumarins' activity is dependent on the substitution pattern situated on ring D. Further investigation revealed that coumarins with a single substitution on this ring exhibit lower activity compared to those with two, and likewise for those with three. The substituted motif type also matters, since it ranks the substituents' activities from most active to least: nitro, chloride, methoxy, methyl, fluoride, cyano, and nitro. In light of these results, the most active of the produced molecules is **TBC9**, featuring three nitro groups on ring D. Our literature review reveals that compounds with nitrobenzene frameworks can target pathogenic anaerobes more effectively. This evidence supports our final verdict.

Table 4. The MIC values of the MET as well as **TBC-p** and its esterified coumarins against pathogenic anaerobes.

Bacterial strain	**Codes of the positive control and TBCs**									
	MET	**TBC-p**	**TBC1**	**TBC2**	**TBC3**	**TBC4**	**TBC5**	**TBC6**	**TBC7**	**TBC8**
B. fragilis	2.85	45.80	6.70	6.55	6.40	4.75	4.70	4.60	4.45	4.40
C. perfringens	0.95	45.45	6.65	6.60	6.65	4.50	4.40	4.35	4.15	4.15
F. necrophorum	1.80	46.35	6.90	6.85	6.70	4.90	4.75	4.70	4.55	4.45
P. melaninogenica	1.05	47.20	6.70	6.75	6.65	4.95	4.90	4.75	4.70	4.75
Bacterial strain	Codes of the TBCs									
	TBC9	**TBC10**	**TBC11**	**TBC12**	**TBC13**	**TBC14**	**TBC15**	**TBC16**	**TBC17**	**TBC18**
B. fragilis	4.35	7.85	7.60	7.45	5.30	5.20	5.05	5.80	5.75	5.60
C. perfringens	4.05	7.75	7.70	7.55	5.30	5.10	4.90	5.90	5.60	5.65
F. necrophorum	4.45	7.75	7.75	7.50	5.50	5.35	5.15	5.95	5.80	5.60
P. melaninogenica	4.70	7.60	7.45	7.35	5.35	5.30	5.25	5.60	5.55	5.45

The μg/ml is the unit used to define the MIC values

Table 5 displays the numbers representing the concentrations at which the MET and the developed coumarins can kill the studied anaerobic bacteria. Also, analyzing these numbers and comparing them with their related MIC numbers shows that they operate in a similar pattern[80]. On the other hand, **Table 6** reveals that these coumarins were bactericidal rather than bacteriostatic against the pathogenic anaerobes under study, since the listed values are less than 4[81].

Table 5. The MBC values of the MET as well as **TBC-p** and its esterified coumarins against pathogenic anaerobes.

Bacterial strain	**Codes of the positive control and TBCs**									
	MET	**TBC-p**	**TBC1**	**TBC2**	**TBC3**	**TBC4**	**TBC5**	**TBC6**	**TBC7**	**TBC8**
B. fragilis	7.90	136.95	19.25	18.20	16.45	12.60	13.55	13.75	11.85	11.65
C. perfringens	2.65	135.85	19.10	18.35	17.15	11.95	12.75	13.05	11.15	11.10
F. necrophorum	5.05	138.50	19.85	19.05	17.25	13.05	13.70	14.10	12.10	11.85
P. melaninogenica	2.90	141.15	19.25	18.80	17.10	13.10	14.15	14.15	12.45	12.65
Bacterial strain	**Codes of the TBCs**									
	TBC9	**TBC10**	**TBC11**	**TBC12**	**TBC13**	**TBC14**	**TBC15**	**TBC16**	**TBC17**	**TBC18**
B. fragilis	12.00	22.65	20.15	21.60	15.25	13.85	11.75	15.45	16.00	16.15
C. perfringens	11.25	22.35	20.40	21.85	15.25	13.50	11.40	15.70	15.65	16.30
F. necrophorum	12.35	22.25	20.55	21.75	15.80	14.20	12.05	15.80	16.10	16.10
P. melaninogenica	13.15	21.85	19.70	21.35	15.45	14.15	12.25	14.90	15.45	15.70

The μg/ml is the unit used to define the MBC values

Table 6. The PM values of the MET as well as **TBC-p** and its esterified coumarins against pathogenic anaerobes.

Bacterial strain	Codes of the positive control and TBCs									
	MET	**TBC-p**	**TBC1**	**TBC2**	**TBC3**	**TBC4**	**TBC5**	**TBC6**	**TBC7**	**TBC8**
B. fragilis	2.772	2.990	2.873	2.776	2.570	2.653	2.883	2.989	2.663	2.648
C. perfringens	2.789	2.989	2.872	2.780	2.579	2.656	2.898	3.000	2.687	2.675
F. necrophorum	2.806	2.988	2.877	2.781	2.575	2.663	2.884	3.000	2.659	2.663
P. melaninogenica	2.762	2.990	2.873	2.785	2.571	2.646	2.888	2.979	2.649	2.663
Bacterial strain	**Codes of the TBCs**									
	TBC9	**TBC10**	**TBC11**	**TBC12**	**TBC13**	**TBC14**	**TBC15**	**TBC16**	**TBC17**	**TBC18**
B. fragilis	2.759	2.885	2.651	2.899	2.877	2.663	2.327	2.664	2.783	2.884
C. perfringens	2.778	2.884	2.649	2.894	2.877	2.647	2.327	2.661	2.795	2.885
F. necrophorum	2.775	2.871	2.652	2.900	2.873	2.654	2.340	2.655	2.776	2.875
P. melaninogenica	2.798	2.875	2.644	2.905	2.888	2.670	2.333	2.661	2.784	2.881

3.4. Activity against pathogenic fungi

Infections caused by fungi are becoming increasingly common and impact millions of individuals across the globe. Athletes' foot, ringworm, and thrush are examples of superficial infections; invasive candidiasis and aspergillosis are illustrations of more serious and potentially fatal diseases[82,83]. People with compromised immune systems, such as chemotherapy patients, transplant recipients, or those with long-term health conditions like diabetes, renal malfunction, or AIDS, are more susceptible to severe fungal infections[84]. The development of antifungal resistance has made it much more difficult to treat aggressive infections once they travel to critical organs. Misdiagnosis, along with therapeutic delays, is common because symptoms are similar to those of other diseases[85]. Environmental fungus, including those responsible for diseases like histoplasmosis and valley fever, can also be a risk to human health in certain areas. To cope with such worries, we need better antifungal drugs, improved hygiene practices, and earlier diagnosis of fungal infections[86].

We evaluated and compared the capacity of our TBCs to inhibit the growth of two fungal strains by calculating their MIC values using the Sabouraud-dextrose broth-microdiluting approach and NYT[87]. We also computed the minimum fungicidal concentration (MFC) measure to determine the chemical concentration capable of killing the fungi under study. Moreover, we quantified these two measures and specified the third one, PM, for each investigated TBC by dividing its MFC value by the MIC[88]. **Table 7** includes the results obtained from the calculation of these three measures, which highlight several conclusive points. One of the key findings is that the TBCs under investigation showed a higher level of activity than NYT against the fungi under study. Also, the **TBC-p** with the carboxylic acid group exhibits the best activity compared with its esterified coumarins. This finding confirms that the esterification of this precursor with phenolic derivatives has minimal impact[89]. However, when we analyzed the activity of the esterified coumarins, we found that those with a high number of substitutions exhibited a higher activity than those with two substitutions, which in turn showed a greater activity than those bearing a single substitution on the ring D. Given the substitution type, the order of activity was chloride, methoxy, methyl, fluoride, cyano, and nitro[90]. On the other hand, the values of the third measure PM suggest that NYT and the synthesized TBCs act as fungicidal antifungal agents; these values fall below the threshold value of 4[91].

Table 7. The MIC, MFC, and PM values calculated for NYT as well as **TBC-p** and their esterified coumarins against pathogenic fungi.

Fungal strain	**MIC (µg/ml)**									
	MET	**TBC-p**	**TBC1**	**TBC2**	**TBC3**	**TBC4**	**TBC5**	**TBC6**	**TBC7**	**TBC8**
C. albicans	5.00	0.95	3.50	3.35	3.20	2.50	2.25	2.15	4.00	4.00
A. niger	9.00	1.15	3.75	3.60	3.55	2.75	2.75	2.70	4.30	4.30
Fungal strain	**MIC (µg/ml)**									
	TBC9	**TBC10**	**TBC11**	**TBC12**	**TBC13**	**TBC14**	**TBC15**	**TBC16**	**TBC17**	**TBC18**
C. albicans	3.90	3.95	3.90	3.75	2.75	2.65	2.60	3.10	2.95	2.80
A. niger	4.15	4.25	4.15	3.95	3.10	3.00	2.90	3.50	3.30	3.25
Fungal strain	**MFC (µg/ml)**									
	MET	**TBC-p**	**TBC1**	**TBC2**	**TBC3**	**TBC4**	**TBC5**	**TBC6**	**TBC7**	**TBC8**
C. albicans	8.00	1.85	10.15	8.35	7.95	7.20	5.50	6.45	11.15	10.60
A. niger	13.00	2.55	10.80	9.00	8.80	7.95	6.70	8.20	11.90	11.45
Fungal strain	MFC (µg/ml)									
	TBC9	**TBC10**	**TBC11**	**TBC12**	**TBC13**	**TBC14**	**TBC15**	**TBC16**	**TBC17**	**TBC18**
C. albicans	10.80	11.40	11.25	10.80	7.95	7.00	6.95	8.60	7.95	8.10
A. niger	11.55	12.20	11.90	11.45	8.90	7.90	7.70	9.70	8.80	9.35
Fungal strain	**PM**									
	MET	**TBC-p**	**TBC1**	**TBC2**	**TBC3**	**TBC4**	**TBC5**	**TBC6**	**TBC7**	**TBC8**
C. albicans	1.600	1.947	2.900	2.493	2.484	2.880	2.444	3.000	2.788	2.667
A. niger	1.444	2.217	2.880	2.500	2.479	2.891	2.436	3.037	2.767	2.667
Fungal strain	**PM**									
	TBC9	**TBC10**	**TBC11**	**TBC12**	**TBC13**	**TBC14**	**TBC15**	**TBC16**	**TBC17**	**TBC18**
C. albicans	2.769	2.886	2.885	2.880	2.891	2.642	2.673	2.774	2.695	2.893
A. niger	2.783	2.871	2.867	2.899	2.871	2.633	2.655	2.771	2.667	2.877

3.5. Biocompatibility with microbiota bacteria

There is a monetary penalty line between treating dangerous infections and ensuring that novel antimicrobial candidates are biocompatible with the bacteria that make up the microbiota[92]. These normal bacteria form an intricate ecology that plays a vital role in our digestion, immune system, and overall well-being[93]. Although antimicrobial drugs are efficient against pathogens, they have the potential to upset this delicate microbial balance. This can result in unforeseen issues, including an increase in dangerous bacteria, infections caused by pathogenic fungi, or disruptions in metabolic processes[94]. Thus, it is critical to evaluate potential novel antimicrobial candidates for biocompatibility with the microbiota to make sure they won't kill off beneficial bacteria, which might affect health in the long run or cause resistance to emerge[95]. To create treatments that effectively treat infections while being safe for the host's general microbial environment, it is crucial to understand how antimicrobial drugs interact with the microbiome[96].

For the reasons mentioned above, we conducted an evaluation on our TBCs to determine their biocompatibility with the normal microbiota. This was done using three normal bacterial strains, CIP, and broth microdiluting as test microorganisms, a reference for comparison, and a method to be used, respectively. **Table 8** presents the values of MIC, MBC, and PM for both the CIP and the synthesized TBCs. By analyzing these numbers, we can identify some conclusive findings. First off, the investigated chemicals demonstrated a bactericidal impact on the normal bacteria under study, with low MIC values for the CIP and high values for

the synthesized TBCs. This finding indicates that the latter chemicals have excellent biocompatibility profiles toward the studied microbiome bacterial strains compared with the reference. In this regard, the values of MIC for the synthesized TBCs can reach about 160-fold higher than those of the CIP[97–99]. There are also small differences between the values of TBCs regarding the three computed microbiological measures. This indicates that the compatibility of TBCs with microbiota bacteria stems from their basic coumarin backbone, not from the esterification and substitution patterns on ring D.

Table 8. The MIC, MFC, and PM values calculated for CIP as well as **TBC-p** and their esterified coumarins toward three different microbiome bacteria.

Microbiome strain	**MIC (µg/ml)**									
	CIP	**TBC-p**	**TBC1**	**TBC2**	**TBC3**	**TBC4**	**TBC5**	**TBC6**	**TBC7**	**TBC8**
E. coli (BAA-1427)	1.05	158	157	158	164	157	159	162	160	157
E. coli (MG1655)	1.85	162	160	160	160	159	166	157	157	158
E. coli (BAA1430)	1.15	155	162	162	163	163	165	158	159	158
Microbiome strain	**MIC (µg/ml)**									
	TBC9	**TBC10**	**TBC11**	**TBC12**	**TBC13**	**TBC14**	**TBC15**	**TBC16**	**TBC17**	**TBC18**
E. coli (BAA-1427)	160	162	157	160	159	160	157	163	158	162
E. coli (MG1655)	160	163	159	163	159	163	157	160	159	164
E. coli (BAA1430)	164	160	155	160	157	167	155	164	155	165
Microbiome strain	**MBC (µg/ml)**									
	CIP	**TBC-p**	**TBC1**	**TBC2**	**TBC3**	**TBC4**	**TBC5**	**TBC6**	**TBC7**	**TBC8**
E. coli (BAA-1427)	3.05	476	472	481	504	476	491	495	494	474
E. coli (MG1655)	5.30	487	482	487	492	482	512	479	484	477
E. coli (BAA1430)	3.30	466	486	493	501	494	509	482	491	477
Microbiome strain	**MBC (µg/ml)**									
	TBC9	**TBC10**	**TBC11**	**TBC12**	**TBC13**	**TBC14**	**TBC15**	**TBC16**	**TBC17**	**TBC18**
E. coli (BAA-1427)	492	495	483	492	491	494	484	502	486	498
E. coli (MG1655)	492	498	489	501	491	503	484	492	489	504
E. coli (BAA1430)	504	488	477	492	484	515	478	505	477	507
Microbiome strain	**PM**									
	CIP	**TBC-p**	**TBC1**	**TBC2**	**TBC3**	**TBC4**	**TBC5**	**TBC6**	**TBC7**	**TBC8**
E. coli (BAA-1427)	2.905	3.013	3.006	3.046	3.073	3.032	3.088	3.056	3.088	3.019
E. coli (MG1655)	2.865	3.006	3.013	3.044	3.075	3.031	3.084	3.051	3.083	3.020
E. coli (BAA1430)	2.870	3.006	3.000	3.043	3.074	3.031	3.085	3.051	3.088	3.019
Microbiome strain	**PM**									
	TBC9	**TBC10**	**TBC11**	**TBC12**	**TBC13**	**TBC14**	**TBC15**	**TBC16**	**TBC17**	**TBC18**
E. coli (BAA-1427)	3.075	3.056	3.076	3.075	3.088	3.088	3.083	3.080	3.076	3.074
E. coli (MG1655)	3.075	3.055	3.075	3.074	3.088	3.086	3.083	3.075	3.075	3.073
E. coli (BAA1430)	3.073	3.050	3.077	3.075	3.083	3.084	3.084	3.079	3.077	3.073

4. Conclusion

This work reports the success in the creation of nineteen TBCs using triclosan as a starting building unit. These coumarins include the precursor **TBC-p** and eighteen of its aromatic esterified coumarins (**TBC1-TBC18**). **Figure 1** shows some intriguing facts about the connection between structure and activity regarding the synthesized TBCs. We discovered these facts by testing them for biocompatibility and antimicrobial activity and then comparing the results with various standards. First, the biocompatibility of the synthesized compounds is entirely dependent on the coumarin framework rather than other structural factors. On the other hand, the antimicrobial activity of the compounds under study depends on the number and type of substitutions in ring D. Given the former factor, compounds with three substituents are more active than those with two, which in turn are more active than those with a single substituent. The type of substitution plays a significant role, with chloride showing the greatest activity against pathogenic aerobic bacteria and nitro showing the greatest activity against pathogenic anaerobic bacteria. **TBC-p** exhibits the highest activity against pathogenic fungi, thereby diminishing the significance of the other two recorded factors. Our recommendation is to direct further studies to utilize these insights for developing more potent and selective antimicrobial prospects derived from the coumarin scaffold.

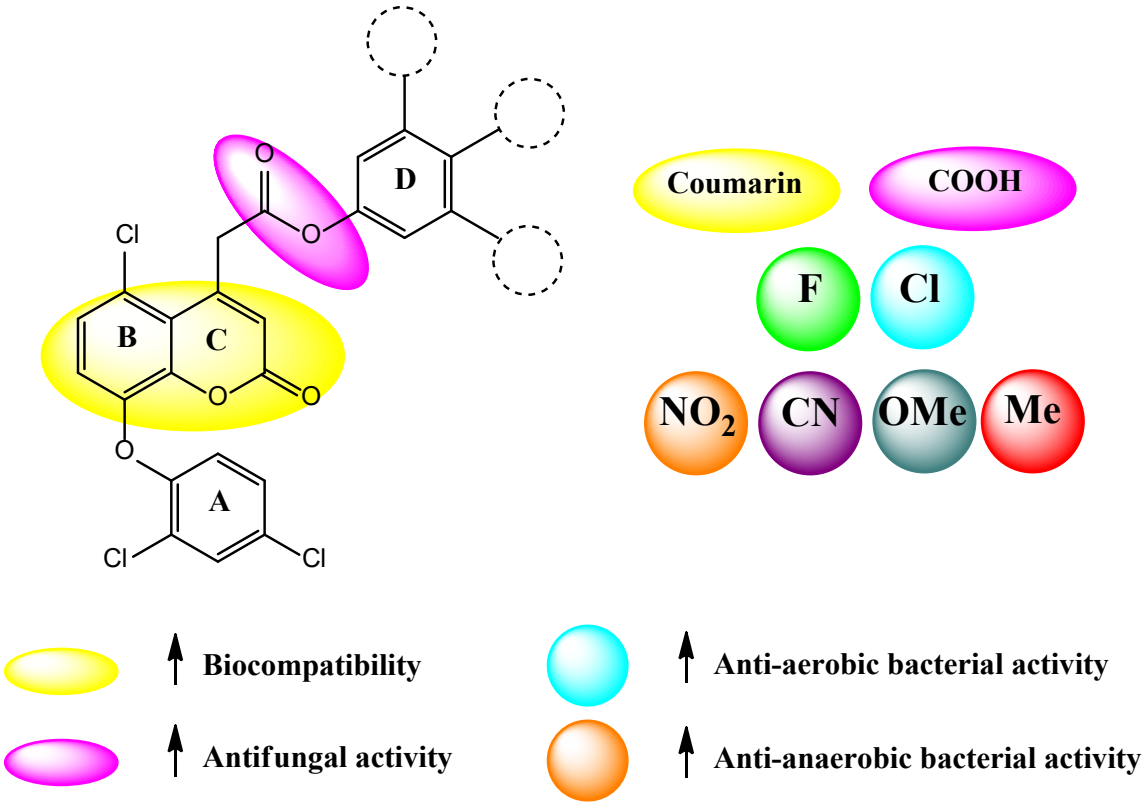

Figure 1. The relationship between the structural characteristics of TBCs and their activity and biocompatibility.

Acknowledgement

The authors are very grateful to the University of Mosul/College of Pharmacy for their provided facilities, which helped to improve the quality of this work.

Funding

The article has not received any funds.

Ethics approval and consent to participates

This article does not contain any studies conducted by any authors of this work. This article does not contain any studies involving patients or animals as test objects.Informed consent was not required for this article.

Conflict of interest

No conflict of interest was declared by the authors.

Author contribution

Both authors have equally contributed to this work.

Data availability

The data that support the findings of this study are available from the corresponding author upon reasonable request.

References

1. Caioni G, Benedetti E, Perugini M, Amorena M, Merola C. Personal Care Products as a Contributing Factor to Antimicrobial Resistance: Current State and Novel Approach to Investigation. Antibiotics 2023;12(4):724.
2. Alfhili MA, Lee MH. Triclosan: An Update on Biochemical and Molecular Mechanisms. Oxidative Medicine and Cellular Longevity 2019;2019:1–28.
3. Ruszkiewicz JA, Li S, Rodriguez MB, Aschner M. Is Triclosan a neurotoxic agent? Journal of Toxicology and Environmental Health, Part B 2017;20(2):104–17.
4. Lee JS, Lee JS, Kim HS. Toxic effects of triclosan in aquatic organisms: A review focusing on single and combined exposure of environmental conditions and pollutants. Science of The Total Environment 2024;920:170902.
5. Weatherly LM, Gosse JA. Triclosan exposure, transformation, and human health effects. Journal of Toxicology and Environmental Health, Part B 2017;20(8):447–69.
6. Sinicropi MS, Iacopetta D, Ceramella J, Catalano A, Mariconda A, Pellegrino M, Saturnino C, Longo P, Aquaro S. Triclosan: A Small Molecule with Controversial Roles. Antibiotics 2022;11(6):735.
7. Mustafa YF, Bashir MK, Oglah MK, Khalil RR, Mohammed ET. Bioactivity of some natural and semisynthetic coumarin derived compounds. NeuroQuantology 2021;19(6):129–38.
8. Waheed SA, Mustafa YF. Benzocoumarin backbone is a multifunctional and affordable scaffold with a vast scope of biological activities. Journal of Medicinal and Chemical Sciences 2022;5(5):703–21.
9. Mustafa YF. Classical approaches and their creative advances in the synthesis of coumarins: A brief review. Journal of Medicinal and Chemical Sciences 2021;4(6):612–25.
10. Bashir MK, Mustafa YF, Oglah MK. Synthesis and antitumor activity of new multifunctional coumarins. Periodico Tche Quimica 2020;17(36):871–83.
11. Jasim SF, Mustafa YF. A Review of Classical and Advanced Methodologies for Benzocoumarin Synthesis. Journal of Medicinal and Chemical Sciences 2022;5(5):676–94.
12. Mustafa YF, Abdulaziza NT, Jasim MH. 4-Methylumbelliferone and its derived compounds: A brief review of their cytotoxicity. Egyptian Journal of Chemistry 2021;64(4):1807–16.
13. Xue L, Singla RK, He S, Arrasate S, González-Díaz H, Miao L, Shen B. Warfarin–A natural anticoagulant: A review of research trends for precision medication. Phytomedicine 2024;128:155479.
14. Bashir MK, Mustafa YF, Oglah MK. Antitumor, antioxidant, and antibacterial activities of glycosyl-conjugated compounds: A review. Systematic Reviews in Pharmacy 2020;11(4):175–87.
15. Mustafa YF, Mohammed ET, Khalil RR. Antioxidant and antitumor activities of methanolic extracts obtained from Red Delicious and Granny Smith apples' seeds. Systematic Reviews in Pharmacy 2020;11(4):570–6.
16. Mustafa YF. Coumarins derived from natural methoxystilbene as oxidative stress-related disease alleviators: Synthesis and in vitro-in silico study. Journal of Molecular Structure 2024;1302:137471.
17. Younes AH, Mustafa YF. Novel coumarins from green sweet bell pepper seeds: Their isolation, characterization, oxidative stress-mitigating, anticancer, anti-inflammatory, and antidiabetic properties. Journal of Molecular Structure 2024;1312:138629.
18. Khalil RR, Mohammed ET, Mustafa YF. Evaluation of in vitro antioxidant and antidiabetic properties of Cydonia Oblonga seeds' extracts. Journal of Medicinal and Chemical Sciences 2022;5(6):1048–58.

19. Mustafa YF. Effects of heat variables on the starch content of cooked white rice: Searching for diabetes-friendly food. Bioactive Carbohydrates and Dietary Fibre 2024;31:100395.
20. Hussein HK, Aubead NM, Kzar HH, Karim YS, Amin AH, Al-Gazally ME, Ahmed TI, Jawad MA, Hammid AT, Jalil AT, Mustafa YF, Saleh MM, Heydari H. Association of cord blood asprosin concentration with atherogenic lipid profile and anthropometric indices. Diabetology & Metabolic Syndrome 2022;14(1):74.
21. Bloh A hameed, Khamis MF, Altekrety AAA, Mustafa YF, Almashhadani HA, Kadhim MM. Total Oxidants, Lipid Peroxidation and Antioxidant Capacity in the Serum of Rheumatoid Arthritis Patients. Journal of Pharmaceutical Negative Results 2022;13(3):231–5.
22. Jebir RM, Mustafa YF. Novel coumarins isolated from the seeds of Citrullus lanatus as potential antimicrobial agents. Eurasian Chemical Communications 2022;4(8):692–708.
23. Mahmood AT, Kamal IK, Mustafa YF. Coumarin Backbone as a Door-Opening Key for Investigating Chloroxylenol as Oral Antimicrobial Agents: an In Vitro–In Silico Study. Russian Journal of Bioorganic Chemistry 2024;50(6):2252–68.
24. Mustafa YF, Mohammed NA alwahab. A promising oral 5-fluorouracil prodrug for lung tumor: Synthesis, characterization and release. Biochemical and Cellular Archives 2021;21(Supp 1):1991–9.
25. Firoozeh AZ, Bokov DO, Salahdin OD, Abdelbasset WK, Jawad MA, Kadhi MM, Qasim MT, Kzar HH, Al-Gazally ME, Mustafa YF, Khatami M. Cytotoxicity evaluation of environmentally friendly synthesis Copper/Zinc bimetallic nanoparticles on MCF-7 cancer cells. Rendiconti Lincei Scienze Fisiche e Naturali 2022;33:441–7.
26. Nejres AM, Ali HK, Behnam SP, Mustafa YF. Potential effect of ammonium chloride on the optical physical properties of polyvinyl alcohol. Systematic Reviews in Pharmacy 2020;11(6):726–32.
27. Mustafa YF, Oglah MK, Bashir MK. Conjugation of sinapic acid analogues with 5- Fluorouracil: Synthesis, preliminary cytotoxicity, and release study. Systematic Reviews in Pharmacy 2020;11(3):482–9.
28. Mustafa YF. Harmful Free Radicals in Aging: A Narrative Review of Their Detrimental Effects on Health. Indian Journal of Clinical Biochemistry 2024;39(2):154–67.
29. Mustafa YF. Coumarins from carcinogenic phenol: synthesis, characterization, in silico, biosafety, anticancer, antioxidant, and anti-inflammatory assessments. Chemical Papers 2024;78:493–504.
30. Mustafa YF. Biocompatible chlorocoumarins from harmful chlorophenols, their synthesis and biomedicinal evaluation. Journal of Molecular Structure 2024;1309:138193.
31. Yahya MQ, Mustafa YF. Transforming Poisonous Phenol into Biosafe Antimicrobial Coumarins: Synthesis and Evaluation. Russian Journal of Bioorganic Chemistry 2024;50(4):1595–608.
32. Mustafa YF, Zain Al-Abdeen SH, Khalil RR, Mohammed ET. Novel functionalized phenyl acetate derivatives of benzo [e]-bispyrone fused hybrids: Synthesis and biological activities. Results in Chemistry 2023;5:100942.
33. Jasim SF, Mustafa YF. Synthesis and Antidiabetic Assessment of New Coumarin-Disubstituted Benzene Conjugates: An In Silico-In Virto Study. Journal of Medicinal and Chemical Sciences 2022;5(6):887–99.
34. Mustafa YF. Synthesis, in silico analysis, and biomedical effects of coumarins derived from resveratrol. Phytomedicine Plus 2024;3(4):100501.
35. Kamal IK, Mahmood AT, Mustafa YF. Synthesis of Eugenol-Derived Coumarins as Broad-Spectrum Biosafe Antimicrobial Agents. Russian Journal of Bioorganic Chemistry 2024;50(6):2240–51.
36. Jasim SF, Mustafa YF. Synthesis, ADME Study, and antimicrobial evaluation of novel naphthalene-based derivatives. Journal of Medicinal and Chemical Sciences 2022;5(5):793–807.
37. Roomi AB, Widjaja G, Savitri D, Jalil AT, Mustafa YF, Thangavelu L, Kazhibayeva G, Suksatan W, Chupradit S, Aravindhan S. SnO2:Au/Carbon Quantum Dots Nanocomposites: Synthesis, Characterization, and Antibacterial Activity. Journal of Nanostructures 2021;11(3):514–23.
38. Mohammed ET, Khalil RR, Mustafa YF. Phytochemical Analysis and Antimicrobial Evaluation of Quince Seeds' Extracts. Journal of Medicinal and Chemical Sciences 2022;5(6):968–79.
39. Mustafaa YF. New Coumarin-Metronidazole Composites: Synthesis, Biocompatibility, and Anti-anaerobic Bacterial Activity. Russian Journal of Bioorganic Chemistry 2024;50(1):201–10.
40. Waheed SA, Mustafaa YF. Novel naphthalene-derived coumarin composites: synthesis, antibacterial, and antifungal activity assessments. Eurasian Chemical Communications 2022;4(8):709–24.
41. Mustafa YF. Combretastatin A4-based coumarins: synthesis, anticancer, oxidative stress-relieving, anti-inflammatory, biosafety, and in silico analysis. Chemical Papers 2024;78:3705–3720.
42. Waheed SA, Mustafa YF. Synthesis and evaluation of new coumarins as antitumor and antioxidant applicants. Journal of Medicinal and Chemical Sciences 2022;5(5):808–19.
43. Jasim SF, Mustafa YF. New fused-coumarin composites: Synthesis, anticancer and antioxidant potentials evaluation. Eurasian Chemical Communications 2022;4(7):607–19.
44. Mustafa YF. Triple coumarin-based 5-fluorouracil prodrugs, their synthesis, characterization, and release kinetics. Journal of Molecular Structure 2024;1301:137415.
45. Waheed SA, Mustafa YF. The in vitro effects of new albocarbon-based coumarins on blood glucose-controlling enzymes. Journal of Medicinal and Chemical Sciences 2022;5(6):954–67.
46. Mustafa YF. 3-mercaptocoumarins as potential bioactive candidates: From novel synthesis to comparative analysis. Journal of Molecular Structure 2025;1320:139657.

47. Mustafa YF. Synthesis of 7,8-dihydroxy-4-phenylbenzo[g]coumarins as potential multitarget anti-skin-aging candidates. Journal of Molecular Structure 2025;1321:139806.
48. Mustafa YF, Hassan DA, Faisal AF, Alshaher MM. Synthesis of novel skipped diene-3-halocoumarin conjugates as potent anticancer and antibacterial biocompatible agents. Results in Chemistry 2024;11:101846.
49. Zeki NM, Mustafa YF. Synthesis of Novel Dioxathiole-6,7-coumarin Hybrids As Cytosafe-Multifunctional Applicants: An In Vitro—In Silico Study. Russian Journal of Bioorganic Chemistry 2024;50(5):2076–91.
50. Mustafa YF. Original Research article Coumarins from toxic phenol: An algorithm of their synthesis and assessment as biosafe, wide-spectrum, potent antimicrobial prospects. Applied Chemical Engineering 2024;7(3):ACE-5527.
51. Jibroo RN, Mustafa YF, Al-Shakarchi W. Heterocycles fused on a 6,7-coumarin framework: an in-depth review of their structural and pharmacological diversity. Chemical Papers 2024;78:7239–7311.
52. Ma X, Wu M, Wang C, Li H, Fan A, Wang Y, Han C, Xue F. The pathogenesis of prevalent aerobic bacteria in aerobic vaginitis and adverse pregnancy outcomes: a narrative review. Reproductive Health 2022;19(1):21.
53. Giannattasio-Ferraz S, Ene A, Gomes VJ, Queiroz CO, Maskeri L, Oliveira AP, Putonti C, Barbosa-Stancioli EF. Escherichia coli and Pseudomonas aeruginosa Isolated From Urine of Healthy Bovine Have Potential as Emerging Human and Bovine Pathogens. Frontiers in Microbiology 2022;13:764760.
54. Mirghani R, Saba T, Khaliq H, Mitchell J, Do L, Chambi L, Diaz K, Kennedy T, Alkassab K, Huynh T, Elmi M, Martinez J, Sawan S, Rijal G. Biofilms: Formation, drug resistance and alternatives to conventional approaches. AIMS Microbiology 2022;8(3):239–77.
55. Devi NS, Mythili R, Cherian T, Dineshkumar R, Sivaraman GK, Jayakumar R, Prathaban M, Duraimurugan M, Chandrasekar V, Peijnenburg WJGM. Overview of antimicrobial resistance and mechanisms: The relative status of the past and current. The Microbe 2024;3:100083.
56. Muteeb G, Rehman MT, Shahwan M, Aatif M. Origin of Antibiotics and Antibiotic Resistance, and Their Impacts on Drug Development: A Narrative Review. Pharmaceuticals 2023;16(11):1615.
57. Hachem K, Jasim SA, Al-Gazally ME, Riadi Y, Yasin G, Turki Jalil A, Abdulkadhm MM, Saleh MM, Fenjan MN, Mustafa YF, Dehno Khalaji A. Adsorption of Pb(II) and Cd(II) by magnetic chitosan-salicylaldehyde Schiff base: Synthesis, characterization, thermal study and antibacterial activity. Journal of the Chinese Chemical Society 2022;69(3):512–21.
58. Jebir RM, Mustafa YF. Watermelon Allsweet: A promising natural source of bioactive products. Journal of Medicinal and Chemical Sciences 2022;5(5):652–66.
59. Jebir RM, Mustafa YF. Natural products catalog of allsweet watermelon seeds and evaluation of their novel coumarins as antimicrobial candidates. Journal of Medicinal and Chemical Sciences 2022;5(5):831–47.
60. Mustafa YF. Emerging trends and future opportunities for coumarin-heterocycle conjugates as antibacterial agents. Results in Chemistry 2023;6:101151.
61. Kotian S, Gupta S, Puttaiahgowda YM, Shetty S. Synthesis and Antibacterial Activity of Grafted Poly(Vinyl Chloride) Polymer against Gram-Positive and Gram-Negative Bacteria. Li W, editor. Advances in Polymer Technology 2024;2024:1–9.
62. Adefisoye MA, Olaniran AO. Does Chlorination Promote Antimicrobial Resistance in Waterborne Pathogens? Mechanistic Insight into Co-Resistance and Its Implication for Public Health. Antibiotics 2022;11(5):564.
63. Contreras Martínez OI, Angulo Ortíz A, Santafé Patiño G. Antibacterial Screening of Isoespintanol, an Aromatic Monoterpene Isolated from Oxandra xylopioides Diels. Molecules 2022;27(22):8004.
64. Zeki NM, Mustafa YF. 6,7-Coumarin-heterocyclic hybrids: A comprehensive review of their natural sources, synthetic approaches, and bioactivity. Journal of Molecular Structure 2024;1303:137601.
65. Ichihashi Y, Sekiguchi T, Hiramatsu K, Tokui Y, Kumagai K, Matsuyama H, Taniya K, Nishiyama S. Applicability and antibacterial activity of polycyclic aromatic compound derivatives used as photocatalysts for water oxidation. Applied Catalysis B: Environmental 2023;325:122326.
66. Zeki NM, Mustafa YF. Annulated Heterocyclic[g]Coumarin Composites: Synthetic Approaches and Bioactive Profiling. Chemistry and Biodiversity 2024;21(3):e202301855.
67. Zeki NM, Mustafa YF. Novel heterocyclic coumarin annulates: synthesis and figuring their roles in biomedicine, bench-to-bedside investigation. Chemical Papers 2024;78:4935–51.
68. Zeki MN, Mustafa YF. Synthesis and evaluation of novel ring-conjugated coumarins as biosafe broad-spectrum antimicrobial candidates. Journal of Molecular Structure 2024;1309:138192.
69. Jibroo RN, Mustafa YF, Al-Shakarchi W. Synthesis and evaluation of linearly fused thiadiazolocoumarins as prospects with broad-spectrum bioactivity. Results in Chemistry 2024;7:101494.
70. Mustafa YF. 4-Chloroskimmetine-based derivatives as potential anticancer and antibacterial prospects: Their synthesis and in vitro inspections. Results in Chemistry 2024;7:101511.
71. Cavallo I, Sivori F, Mastrofrancesco A, Abril E, Pontone M, Di Domenico EG, Pimpinelli F. Bacterial Biofilm in Chronic Wounds and Possible Therapeutic Approaches. Biology 2024;13(2):109.
72. Mustafa YF. Modern Developments in the Application and Function of Metal/Metal Oxide Nanocomposite–Based Antibacterial Agents. BioNanoScience 2023;13:840–52.

73. Ranjbar M, Salehi R, Haghjooy Javanmard S, Rafiee L, Faraji H, Jafarpor S, Ferns GA, Ghayour-Mobarhan M, Manian M, Nedaeinia R. The dysbiosis signature of Fusobacterium nucleatum in colorectal cancer-cause or consequences? A systematic review. Cancer Cell International 2021;21(1):194.
74. Mustafa YF. Chemotherapeutic applications of folate prodrugs: A review. NeuroQuantology 2021;19(8):99–112.
75. Le Vavasseur B, Zeller V. Antibiotic Therapy for Prosthetic Joint Infections: An Overview. Antibiotics 2022;11(4):486.
76. Younes HA, Mustafa YF. Sweet Bell Pepper: A Focus on Its Nutritional Qualities and Illness-Alleviated Properties. Indian Journal of Clinical Biochemistry 2024;39:459–69.
77. Mustafa YF. Synthesis of novel 6-aminocoumarin derivatives as potential –biocompatible antimicrobial and anticancer agents. Journal of Molecular Structure 2025;1320:139658.
78. Younes AH, Mustafa YF. Plant-Derived Coumarins: A Narrative Review Of Their Structural And Biomedical Diversity. Chemistry & Biodiversity 2024;21(6):e202400344.
79. Zeki NM, Mustafa YF. Coumarin hybrids: a sighting of their roles in drug targeting. Chemical Papers 2024;78:5753–5772.
80. Abdulaziz NT, Mustafa YF. Antibacterial and Antitumor Potentials of Some Novel Coumarins. International Journal of Drug Delivery Technology 2022;12(1):239–47.
81. Zeki NM, Mustafa YF. Digital alchemy: Exploring the pharmacokinetic and toxicity profiles of selected coumarin-heterocycle hybrids. Results in Chemistry 2024;10:101754.
82. Ismael RN, Mustafa YF, Al-Qazaz HK. Citrullus lanatus, a Potential Source of Medicinal Products: A Review. Journal of Medicinal and Chemical Sciences 2022;5(4):607–18.
83. Jasim SA, Abdelbasset WK, Shichiyakh RA, Al-Shawi SG, Yasin G, Jalil AT, Karim YS, Mustafa YF, Norbakhsh M. Probiotic effects of the fungi, Aspergillus niger on growth, immunity, haematology, intestine fungal load and digestive enzymes of the common carp, Cyprinus carpio. Aquaculture Research 2022;53(10):3828–40.
84. Loh JT, Lam KP. Fungal infections: Immune defense, immunotherapies and vaccines. Advanced Drug Delivery Reviews 2023;196:114775.
85. Al Abdeen SHZ, Mustafa YF, Mutlag SH. Synthesis and biomedical activities of novel multifunctional benzodipyrone-based derivatives. Eurasian Chemical Communications 2022;4(10):938–49.
86. Denham ST, Wambaugh MA, Brown JCS. How Environmental Fungi Cause a Range of Clinical Outcomes in Susceptible Hosts. Journal of Molecular Biology 2019;431(16):2982–3009.
87. Zeki NM, Mustafa YF. Natural linear coumarin-heterocyclic conjugates: A review of their roles in phytotherapy. Fitoterapia 2024;175:105929.
88. Zeki NM, Mustafa YF. Coumarin hybrids for targeted therapies: A promising approach for potential drug candidates. Phytochemistry Letters 2024;60:117–33.
89. Xun W, Gong B, Liu X, Yang X, Zhou X, Jin L. Antifungal Mechanism of Phenazine-1-Carboxylic Acid against Pestalotiopsis kenyana. International Journal of Molecular Sciences 2023;24(14):11274.
90. Younes AH, Mustafa YF. Unveiling the Biomedical Applications of Novel Coumarins Isolated From Capsicum Annuum L. Seeds by a Multivariate Extraction Technique. Chemistry and Biodiversity 2024;21(6):e202400581.
91. Conn BN, Lieberman JA, Chatman P, Cotton K, Essandoh MA, Ebqa'ai M, Nelson TL, Wozniak KL. Antifungal activity of eumelanin-inspired indoylenepheyleneethynylene against Cryptococcus neoformans. Frontiers in Microbiology 2024;14:1339303.
92. Mustafa YF, Ismael RN, Jebir RM. Natural coumarins from two cultivars of watermelon seeds as biosafe anticancer agents, an algorithm for their isolation and evaluation. Journal of Molecular Structure 2024;1295(P1):136644.
93. Mustafa YF, Khalil RR, Mohammed ET. Antimicrobial activity of aqueous extracts acquired from the seeds of two apples ' cultivars. Systematic Reviews in Pharmacy 2020;11(2):382–7.
94. Mancuso G, Midiri A, Gerace E, Biondo C. Bacterial Antibiotic Resistance: The Most Critical Pathogens. Pathogens 2021;10(10):1310.
95. Mustafa YF, Abdulaziz NT. Biological potentials of hymecromone-based derivatives: A systematic review. Systematic Reviews in Pharmacy 2020;11(11):438–52.
96. Aldewachi H, Mustafa YF, Najm R, Ammar F. Adulteration of slimming products and its detection methods. Systematic Reviews in Pharmacy 2020;11(3):289–96.
97. Al-Shakarchi W, Saber Y, Merkhan M, Mustafa Y. ACUTE TOXICITY OF COUMACINES: AN IN VIVO STUDY. Georgian medical news 2023;(338):126–31.
98. Al-Shakarchi W, Saber Y, Merkhan MM, Mustafa YF. Sub Chronic Toxicity Study of Coumacines. Pharmacognosy Journal 2023;15(1):160–4.
99. Younis MA, Hamid OA, Dhaher R, Saber Y, Al-shakarchi W, Merkhan MM, Mustafa YF. Characterization of the renal safety profiles of coumacines. Pharmakeftiki 2023;35(4):57–63.